Analysis of Power-Law Fluid Flow in a Microchannel with Electrokinetic Effects

Cunlu Zhao and Chun Yang
School of mechanical and aerospace engineering, Nanyang Technological University,
50 Nanyang Avenue, 639798, Singapore
E-mail: mcyang@ntu.edu.sg

Abstract
The pressure driven flow of power-law fluids in microchannels subject to electrokinetic effects is analyzed in this work. The Cauchy momentum equation together with the power-law fluid constitutive equation is used to describe the power-law fluid flow in a slit microchannel with consideration of a body force resulting from the interaction of the charge density in the electrical double layer of the channel and the flow-induced electrokinetic potential. By using an appropriate approximate scheme, an expression for the induced streaming potential is obtained. The velocity profile, volumetric flow rate, apparent viscosity and friction coefficient are analytically evaluated, and the influencing factors including ionic concentration, wall zeta potential, flow behavior index and pressure difference are investigated. It is found that the pseudoplastic fluids are more susceptible to electokinetic effects than the dilatant fluids and then the flow characteristics of the pseudoplastic fluids are found to deviate drastically from those of Newtonian fluids.

Keywords: Electrokinetic effects; Power-law fluids; Microchannel flow

NOMENCLATURE

a_n, b_n, c_n	Coefficients for the quadratic equation of streaming potential with arbitrary flow behavior index
$a_{1/2}$, $b_{1/2}$, $c_{1/2}$	Coefficients for the quadratic equation of streaming potential with a flow behavior index of 1/2
b_1, c_1	Coefficients for the linear equation of streaming potential for Newtonian fluids
C_f	Friction coefficient
D_h	Hydraulic diameter [m]
e	Charge of a proton[C]
E_x	Electrical field strength along the horizontal direction [V/m]
$F(n, x)$, $F_1(n, x)$, $F_2(n, x)$, $F_3(n, x)$	Auxiliary functions
G_1, G_2	Non-dimensional parameters
H	Half of channel height [m]
$H(n, x)$, $H_1(n, x)$ $H_2(n, x)$	Auxiliary functions
I_c, I_s	Conduction and streaming current, respectively [A]
k_B	Boltzmann's constant [J/K]
m	Flow consistency index [Pages^n]
n	Flow behavior index
n_∞	Bulk number concentration of the ions[/m^3]
p	Pressure [Pa]

P_x	Pressure gradient along the x direction[Pa/m]
Q, Q_0	Volumetric flow rate with and without *EDL* effects, respectively[m^3/s]
Re	Reynolds number
T	Absolute temperature [K]
v_x	Local velocity in the axial direction [m/s]
V_{av}, V_{av0}	Mean velocity with and without *EDL* effects, respectively[m/s]
V, V_0	Reference velocities [m/s]
x, y	Cartesian coordinates [m]
Y	Non-dimensional y coordinate
z	Valence of ions

Greek symbols

ε	Dielectric constant = ε_r, ε_0 [F/m]
ε_r	Relative permittivity
ε_0	Vacuum permittivity[F/m]
Γ	Magnitude of rate-of-strain tensor [m^2/s]
$\Gamma(\alpha,\xi)$	Incomplete Gamma function
κ	The Debye-Hückel parameter [m^{-1}]
$\lambda_b, \lambda_s, \lambda_t$	Electrical conductivity of the solution, surface conductivity, total electrical conductivity, respectively[$S \bullet m^{-1}$]
μ_a, μ_{a0}	Apparent dynamic viscosity of power-law fluids with and without *EDL* effects, respectively [$Pa \bullet s$]
ρ	Fluid density [kg/m^3]
ρ_e	Net charge density [C/m^3]
ψ, ψ_w	*EDL* potential distribution and zeta potential of the microchannel wall, respectively[V]
Ψ, Ψ_w	Nondimensional *EDL* potential distribution and zeta potential of the microchannel wall, respectively
ζ_0	Reference potential [V]

Bold symbols

$\boldsymbol{F}$	Body force vector
$\mathbf{\Gamma}$	Rate-of-strain tensor
$\mathbf{v}$	Velocity vector

1. INTRODUCTION

Liquid flow through microchannels has found its applications in microfluidic devices, ranging from pH and temperature sensors, to fluid actuators, such as pumps, mixers, and valves[1], as well as Lab-on-a-Chip systems for drug delivery, chemical analysis, and biomedical diagnosis[2]. Understanding of flow physics in microchannels is of great importance to the successful and optimal design and precise control of microfluidic devices. However, the existing theories cannot be scaled down to describe completely the flow in microchannels, where some surface phenomena such as capillary, wetting, electrokinetic effects, can cause the flow characteristics to deviate from those in large-sized channels.

In the literature, numerous theoretical studies were reported to explain the deviation of microscale flow characteristics; the micro-polar fluid theory[3], the micro-moment theory[4], and the electrokinetics[5] are a few to name. In this study, the electrokinetic effects are considered. It is known that most solid surfaces acquire electrostatic charges, i.e., an electrical surface potential. The presence of such charges would cause the redistribution of ions in the neighborhood of the charged surface, leading to the development of a so-called electrical double layer (*EDL*). An *EDL* consists of an immobile compact layer and a mobile diffuse layer where there are more counter-ions than co-ions and hence the net charge density is not zero. When a liquid is forced through a microchannel under an applied hydrostatic pressure, more counter-ions in the diffuse layer are carried towards the downstream to form a streaming current, along the direction of the liquid flow. Meanwhile, the accumulation of counter-ions in the downstream end builds up an electric field with a streaming potential which in turn generates a conduction current, in the opposite direction of the flow. When the conduction current equals the streaming current, a steady state is reached. It is easy to comprehend that the streaming potential would exert electrostatic resistant force on the net charge density in the diffuse layer, thereby hinder the pressure-driven flow, which is also termed as the electroviscous effects. The electroviscous effects become significant for liquid flow in a microchannel where the thickness of the *EDL* is often comparable with the channel dimension.

The electrokinetic effects on microchannel flow have been experimentally studied by Mala et al.[6], Ren et al.[7], Kulinsky et al.[8] and Brutin and Tadrist[9]. Their results showed that depending on the channel height and the electrical properties of the channel surface, the measured flow rate of the distilled water can be 80% lower than that predicted from the classical Poiseuille flow equation. The electroviscous effects have also been theoretically studied for slit-like channels (Mala et al.[10], Chun and Kwak[11]) and for rectangular channels (Yang and Li[12, 13], Yang et al.[14]). In these studies, the electrokinetic effects on velocity distribution, friction coefficient, apparent viscosity, and heat transfer were examined. Their analyses predicted that the electrokinetic effects can result in a higher friction coefficient, a larger apparent viscosity, and a reduced Nusselt number.

However, all the forenamed studies are concerned with the flow of Newtonian fluids in microchannels. Microfluidic devices are usually used to analyze biofluids which may not be treated as Newtonian fluids. For non-Newtonian fluids, the flow field should be governed by the general Cauchy momentum equation, instead of the Navier-Stokes equation. Numerous models such as Power-law model[15], Carreau model[16], Moldflow first-order model[17], and Bingham model[18] have been proposed to describe the correlation between the shear stress and the rate of strain tensor. However few studies have been reported for the flow of non-Newtonian fluids in microchannels. Das and Chakraborty[19] considered the electroosmotic flow of power-law fluids in a slit. Zimmerman et al.[16] studied the electrokinetic flow of Carreau fluids in a T-shaped microchannel. Berli and Olivares[20] analyzed the wall depletion effect on flow of non-Newtonian fluids by extending the general force-flux relations for simple fluids to non-Newtonian fluids. More recently, Zhao et al.[21] derived a generalized Smoluchowski slip velocity for electroosmotic flow of power-law fluids.

In this work, the electrokinetic effects on pressure driven flow of power-law fluids in a microchannel are studied. The flow field of power-law fluids is governed by the general Cauchy momentum equation with consideration of a body force originating from the interaction of the net charge density in the channel *EDL* and the induced electrokinetic streaming potential. Analytical expressions are obtained for the velocity distribution, volumetric flow rate, apparent viscosity and friction coefficient. Parametric studies of the electrokinetic effects on flow of power-law fluids in a microchannel under the influence of the ionic concentration, wall zeta potential, flow behavior index and pressure difference are performed.

2. POWER-LAW FLUIDS AND GENERAL GOVERNING EQUATIONS

For non-Newtonian fluids, the viscous stress is not a linear function of the rate of strain tensor. The magnitude of the rate of strain tensor is defined as[22]

$$\Gamma \equiv [\frac{1}{2}(\mathbf{\Gamma} : \mathbf{\Gamma})]^{1/2} \tag{1}$$

where $\mathbf{\Gamma}$ is the rate of strain tensor and Γ is its magnitude. The fluid viscosity can be expressed as a function of the above defined scalar, namely $\mu(\Gamma)$. The present work concerns a specific non-Newtonian fluid termed as the power-law fluid whose dynamic viscosity, μ, is described by[22]

$$\mu = m(2\Gamma)^{n-1} \tag{2}$$

where m is the flow consistency index, and n is the flow behavior index which represents an apparent or effective viscosity being a function of the shear rate. Shear-thinning (also termed as pseudoplastic) behavior is obtained for $n < 1$, and it indicates that the fluid viscosity decreases with increasing rate of shear. Pseudoplasticity can be demonstrated by the manner in which shaking a bottle of ketchup causes the contents to undergo an unpredictable change in viscosity. Newtonian behavior is obtained for $n = 1$. Shear-thickening (also termed as dilatant) behavior is obtained for $n > 1$, and it shows that the fluid viscosity increases with the rate of shear. The dilatant effect can readily be seen with a mixture of cornstarch and water, which acts in counter-intuitive ways when struck or thrown against a surface.

The flow field of the power-law fluids is governed by the continuity equation and the Cauchy momentum equation. For an incompressible fluid, the continuity equation can be written as[22]

$$\nabla \bullet \mathbf{v} = 0 \tag{3}$$

where $\mathbf{v}$ is the velocity vector. Using a general relationship between the viscous stress tensor and the rate of strain tensor, given by eqn (4),

$$\tau = 2\mu(\Gamma)\mathbf{\Gamma} = \mu(\Gamma)[\nabla\mathbf{v} + (\nabla\mathbf{v})^T] \tag{4}$$

we can write the Cauchy momentum equation as[22]

$$\rho\frac{D\mathbf{v}}{Dt} = -\nabla p + \boldsymbol{F} + \nabla \bullet \left\{\mu(\Gamma)[\nabla\mathbf{v} + (\nabla\mathbf{v})^{\mathrm{T}}]\right\} \tag{5}$$

where ρ is the density, p is the pressure, $\boldsymbol{F}$ is the body force vector, $\nabla\mathbf{v}$ is the velocity gradient tensor and $(\nabla\mathbf{v})^T$ is the transpose of velocity gradient tensor.

3. FLOW FIELD OF POWER-LAW FLUIDS IN A SLIT MICROCHANNEL

Consider a slit microchannel of height $2H$ and length L as illustrated in Figure 1. The channel is filled with an incompressible, power-law electrolyte of constant dielectric constant ε, flow consistency index m, and flow behavior index n. The slit wall is assumed to be uniformly charged with a zeta potential ψ_w. Because of geometric symmetry, the analysis is restricted in the upper half domain of the slit microchannel.

When a pressure difference is applied along the microchannel, the liquid flow is governed by the Cauchy momentum eqn (5). For a steady, fully developed flow, the components of $\mathbf{v}$ satisfy $v_x = v_x(y)$ and $v_y = v_z = 0$. The hydraulic pressure gradient is a constant. Therefore, the material derivative of $\mathbf{v}$ with respect to time vanishes and the continuity equation is automatically satisfied. Furthermore, with negligible gravitational force, the only body force considered here is due to the interaction of the net charge density in the channel *EDL* ρ_e and the induced streaming potential E_x. Such force acts only along x direction, and is given by

$$F_x = E_x\rho_e \tag{6}$$

When the wall zeta potential ψ_w is small, the net charge density ρ_e can be expressed as a function of the *EDL* potential[23]

$$\rho_e(y) = -\kappa^2\,\varepsilon\psi \tag{7}$$

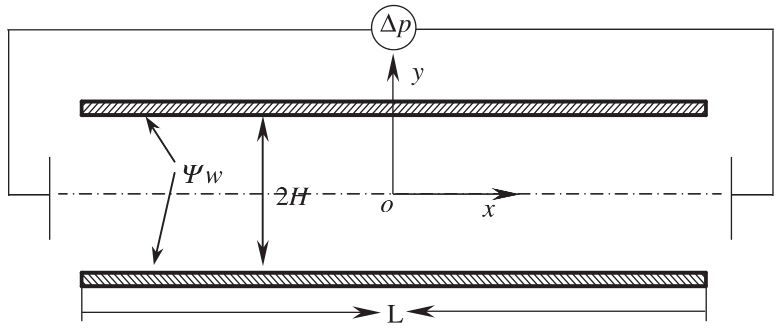

Figure 1. Schematic configuration of a microchannel slit with height of $2H$ and length of L, and with a uniform zeta potential of ψ_w.

where κ^{-1} is termed as the Debye length, and is defined as $\kappa^{-1} = (\varepsilon k_B T/2e^2 z^2 n_\infty)^{1/2}$ (here n_∞ and z are the bulk number concentration and the valence of ions, respectively, e is the fundamental charge, k_B is the Boltzmann constant, and T is the absolute temperature). An expression for the *EDL* potential distribution is of the following form[23]

$$\psi(y) = \psi_w \frac{\cosh(\kappa y)}{\cosh(\kappa H)} \tag{8}$$

Defining the dimensionless groups: $K=\kappa H$, $Y=y/H$ and $\psi=ze\Psi/k_b T$, we can nondimensionalize eqn (8) as

$$\Psi(Y) = \Psi_w \frac{\cosh(KY)}{\cosh(K)} \tag{9}$$

Recalling that the magnitude of the rate of strain tensor in this case is expressed as $\Gamma = (1/2)\, |dv_x/dy|$, we can obtain an expression for the viscosity using eqn (2),

$$\mu = m(-\frac{dv_x}{dy})^{n-1} \tag{10}$$

where the negative sign is chosen because the velocity decreases with increasing y in the channel.

Therefore, we can show that the Cauchy momentum eqn (5) can be simplified to

$$-\frac{dp}{dx} + \frac{d}{dy}[m(-\frac{dv_x}{dy})^{n-1}\frac{dv_x}{dy}] - \kappa^2 \varepsilon E_x \psi = 0 \tag{11}$$

By introducing the following dimensionless parameters,

$$\bar{v} = \frac{v_x}{V} \quad \bar{P}_x = \frac{H}{\rho V^2}\frac{dp}{dx} \quad \bar{E}_x = \frac{E_x H}{\zeta_0} \quad \bar{G}_1 = \frac{2zen_\infty \zeta_0}{\rho V^2} \quad V = \frac{n}{n+1}\left(-\frac{1}{m}\frac{dp}{dx}\right)^{\frac{1}{n}} H^{\frac{n+1}{n}} \tag{12}$$

we can obtain eqn (13) that gives the dimensionless form of eqn (11),

$$(\frac{n+1}{n})^n - \frac{d}{dY}[(-\frac{d\bar{v}}{dY})^n] - (\frac{n+1}{n})^n(-\bar{P}_x)^{-1}\bar{G}_1\bar{E}_x\Psi = 0 \tag{13}$$

where V is the centerline velocity without consideration of the *EDL* effect and ζ_0 is a reference electrical potential. Eqn (13) can be solved using the following boundary conditions

$$\bar{v}\big|_{Y=1} = 0 \qquad \frac{d\bar{v}}{dY}\bigg|_{Y=0} = 0 \tag{14}$$

An analytical solution of eqn (13) can be obtained as

$$\bar{v}(Y) = \frac{n+1}{n}(-\bar{P})^{-\frac{1}{n}}\int_Y^1[(-\bar{P}_x)Y' - \frac{\bar{G}_1\bar{E}_x\Psi_w}{K}\frac{\sinh(KY')}{\cosh(K)}]^{\frac{1}{n}}dY' \tag{15}$$

Eqn (15) shows that the flow is retarded due to the induced streaming potential. The integral can be carried out analytically only for specific values of the flow behavior index n, such as 1, $\frac{1}{2}$, and $\frac{1}{3}$ etc.

Specific Cases:

The case of $n = 1$ corresponds to Newtonian fluids where $m = \mu$, and eqn (15) can be evaluated as

$$\bar{v}(Y) = (1 - Y^2) - 2(-\bar{P}_x)^{-1}\bar{G}_1\Psi_w\bar{E}_x\frac{\cosh(K) - \cosh(KY)}{K^2\cosh(K)} \tag{16}$$

When $n = \frac{1}{2}$, we can show that the dimensionless velocity can be expressed as

$$\bar{v}(Y) = (1 - Y^3) + 3(-\bar{P}_x)^{-2}(\bar{G}_1\Psi_w\bar{E}_x)^2 \frac{[\sinh(2K) - \sinh(2KY)] - 2(K - KY)}{4K^3\cosh^2(K)} - 3(-\bar{P}_x)^{-1}\bar{G}_1\Psi_w\bar{E}_x \frac{2\{[K\cosh(K) - KY\cosh(KY)] - [\sinh(K) - \sinh(KY)]\}}{K^3\cosh(K)} \tag{17}$$

Approximate Analytical Solution:

As the integral in eqn (15) can be analytically evaluated only under certain circumstances, in the following we will present an approximate approach to obtain the velocity distributions from eqn (15). It is assumed that in eqn (15) the actuating pressure force term is much larger than the induced electrostatic body force term due to electrokinetic effects, and thus we have the following assumption

$$\frac{\dfrac{\bar{G}_1\Psi_w\bar{E}_x}{K}\dfrac{\sinh(KY')}{\cosh(K)}}{(-\bar{P}_x)Y'} = 1 \tag{18}$$

Using Taylor's series for $|x| \approx 1$and an arbitrary real number η, we have

$$\left(1 + x\right)^{\eta} \approx 1 + \eta x + \frac{\eta\left(\eta - 1\right)}{2}x^2 + \ldots\ldots \tag{19}$$

Therefore, eqn (15) can be analytically integrated using the approximations in eqns (18) and (19),

$$\begin{aligned}\bar{v}(Y) &= \frac{n+1}{n}(-\bar{P}_x)^{-\frac{1}{n}}\int_Y^1[(-\bar{P}_xY')^{\frac{1}{n}} - \frac{1}{n}\frac{\bar{G}_1\bar{E}_x\Psi_w}{K}(-\bar{P}_xY')^{\frac{1}{n}-1}\frac{\sinh(KY')}{\cosh(K)} \\ &+ \frac{1-n}{2n^2}\frac{\bar{G}_1{}^2\bar{E}_x^2\Psi_w^2}{K^2}(-\bar{P}_xY')^{\frac{1}{n}-2}\frac{\sinh^2(KY')}{\cosh^2(K)}]dY' \\ &= (1 - Y^{\frac{n+1}{n}}) - \frac{n+1}{n^2}(-\bar{P}_x)^{-1}\bar{G}_1\Psi_w\bar{E}_x\frac{F(n,K) - F(n,KY)}{K^{\frac{n+1}{n}}\cosh(K)} \\ &+ \frac{1-n^2}{2n^3}(-\bar{P}_x)^{-2}\bar{G}_1^2\Psi_w^2\bar{E}_x^2\frac{H(n,K) - H(n,KY)}{K^{\frac{n+1}{n}}\cosh^2(K)}\end{aligned} \tag{20}$$

where the two auxiliary functions, i.e., $F(n, x)$ and $H(n, x)$, are defined in Appendix. Likewise, all other auxiliary functions, including $F_1(n, x)$, $F_2(n, x)$, $F_3(n, x)$, $H_1(n, x)$ and $H_2(n, x)$, used in the following are also defined in Appendix without otherwise specified.

In the case of no electrokinetic effects, the second term and third term on the right hand side of eqn (20) vanish. Eqn (20) reduces to

$$\bar{v}_0(Y) = 1 - Y^{\frac{n+1}{n}} \tag{21}$$

which is the well-known pressure-driven flow velocity profile of power-law fluids through a parallel-plate channel.

Using eqns (20) and (21), we can show that the mean velocity with and without the consideration of the electrokinetic effects respectively are

$$\bar{V}_{av} = \int_0^1 \bar{v}\left(Y\right) dY = \frac{n+1}{2n+1} - \frac{n+1}{n^2}\left(-\bar{P}_x\right)^{-1} \bar{G}_1 \Psi_w \bar{E}_x \frac{KF\left(n,K\right) - \left[F_1\left(n,K\right) - F_1\left(n,0\right)\right]}{K^{\frac{2n+1}{n}} \cosh(K)}$$
$$+ \frac{1-n^2}{2n^3}\left(-\bar{P}_x\right)^{-2} \bar{G}_1^2 \Psi_w^2 \bar{E}_x^2 \frac{KH\left(n,K\right) - \left[H_1\left(n,K\right) - H_1\left(n,0\right)\right]}{K^{\frac{2n+1}{n}} \cosh^2\left(K\right)} \tag{22}$$

and

$$\bar{V}_{av0} = \int_0^1 v_0\left(Y\right) dY = \frac{n+1}{2n+1} \tag{23}$$

Hence, the non-dimensional volumetric flow rate through the slit microchannel, defined by $\bar{Q} = Q/(2HV_0)$, is given by

$$\bar{Q} = \frac{V}{V_0}\bar{V}_{av} \tag{24}$$

Here another constant reference velocity V_0 is adopted instead of using the reference velocity V introduced earlier. The reason is that we usually want to examine the effects of pressure gradient and flow behavior index on the flow rate, but the reference velocity V already includes the pressure gradient and flow behavior index. Correspondingly, in the absence of the electrokinetic effects, the non-dimensional volumetric flow rate is expressed as

$$\bar{Q}_0 = \frac{V}{V_0}\bar{V}_{av0} \tag{25}$$

4. STREAMING POTENTIAL

As seen from eqns (20) and (22), the local and mean velocity can be evaluated only when the induced streaming potential $\bar{E}_x$ is known. As explained previously, under a steady-state condition, the conduction current I_c is equal to the streaming current I_s, and the net electrical current I should be zero

$$I = I_s + I_c = 0 \tag{26}$$

Due to symmetry of the microchannel, the electrical streaming current I_s is defined as

$$I_s = 2\int_0^H v_x(y)\rho_e dy = -4ezn_\infty HV\int^1 \bar{v}(Y)\Psi dY \tag{27}$$

The electrical conduction current I_c in the microchannel consist of two parts: one is due to the conductance of the bulk liquid; the other is due to the surface conductance of the compact layer of the *EDL*. The electrical conductance current can be expressed as

$$I_c = I_{bc} + I_{sc} = \lambda_t E_x A_c = 2\lambda_t \zeta_0 \bar{E}_x \tag{28}$$

where I_{bc}, I_{sc} represent the bulk and surface conductance current respectively. λ_t is the total electrical conductivity and it can be calculated by $\lambda_t = \lambda_b + \lambda_s P_s / A_c$. Here P_s and A_c are the wetting perimeter and the cross-sectional area of the channel, respectively. λ_b is the bulk conductivity of the solution, and λ_s is the surface conductivity, which may be determined by experiment[6].

From eqns (26), (27) and (28), we can obtain an expression for the streaming potential

$$\bar{E}_x = \bar{G}_2 \int_0^1 \bar{v}(Y)\Psi dY \tag{29}$$

Here we introduce a dimensionless parameter, $\bar{G}_2 = 2zen_\infty HV/(\lambda_t \zeta_0)$.

Using the velocity distribution (i.e., eqn (20)) and the *EDL* potential profile (i.e., eqn (9)), we can show that the streaming potential satisfies the following quadratic equation

$$a_n \bar{E}_x^2 - (1 + b_n)\,\bar{E}_x + c_n = 0 \tag{30}$$

where three constant coefficients a_n, b_n, and c_n are given by

$$a_n = \frac{1-n^2}{2n^3}\bar{G}_1\bar{G}_2(-\bar{P}_x)^{-2}\Psi_w^3 \frac{\sinh(K)H(K,n) - [H_2(n,K) - H_2(n,0)]}{K^{\frac{2n+1}{n}}\cosh^3(K)} \tag{31a}$$

$$b_n = \frac{n+1}{n^2}\bar{G}_1\bar{G}_2(-\bar{P}_x)^{-1}\Psi_w^2 \frac{\sinh(K)F(K,n) - [F_2(n,K) - F_2(n,0)]}{K^{\frac{2n+1}{n}}\cosh^2(K)} \tag{31b}$$

$$c_n = \bar{G}_2\Psi_w \frac{K^{\frac{n+1}{n}}\sinh(K) - [F_3(n,K) - F_3(n,0)]}{K^{\frac{2n+1}{n}}\cosh(K)} \tag{31c}$$

Then the dimensionless streaming potential can be determined by using eqn (32)

$$\bar{E}_x = \begin{cases} \dfrac{(1+b_n) - \sqrt{(1+b_n)^2 - 4a_n c_n}}{2a_n} & n \neq 1 \\[2ex] \dfrac{c_n}{1+b_n} & n = 1 \end{cases} \tag{32}$$

Recall that in the previous section, the exact solutions of the velocity distributions are already obtained for the flow index, n=1 and $\frac{1}{2}$. Therefore, the exact solutions of the streaming potential for these two cases can also be found. For Newtonian fluids when n=1, substituting eqns (16) and (9) into eqn (29), we can show that the streaming potential satisfies a linear equation as follow

$$-(b_1 + 1)\bar{E}_x + c_1 = 0 \tag{33}$$

where

$$b_1 = \bar{G}_1\bar{G}_2(-\bar{P}_x)^{-1}\Psi_w^2 \frac{\cosh(K)\sinh(K) - K}{K^3\cosh^2(K)} \tag{34a}$$

$$c_1 = 2\overline{G_2}\Psi_w \frac{K\cosh(K) - \sinh(K)}{K^3\cosh(K)} \tag{34b}$$

The exact solution of the streaming potential can be readily evaluated from eqn (33)

$$\bar{E}_x = \frac{c_1}{b_1 + 1} \tag{35}$$

Likewise, for n=$\frac{1}{2}$, it can be shown that by substituting eqns (17) and (9) into eqn (29), we can have the following quadric equation,

$$a_{1/2}\bar{E}_x^2 - (b_{1/2} + 1)\bar{E}_x + c_{1/2} = 0 \tag{36}$$

where

$$a_{1/2} = 3\bar{G}_1\bar{G}_2(-\bar{P}_x)^{-2}\Psi_w^3 \frac{\sinh(2K)\sinh(K) - \frac{1}{6}\cosh(3K) - \frac{5}{2}\cosh(K) + \frac{8}{3}}{4K^4\cosh^3(K)} \quad (37a)$$

$$b_{1/2} = 3\bar{G}_1\bar{G}_2(-\bar{P}_x)^{-1}\Psi_w^2 \frac{K\sinh(2K) - \sinh^2(K) - K^2}{2(K)^4\cosh^2(K)} \quad (37b)$$

$$c_{1/2} = 3\bar{G}_2\Psi_w \frac{K^2\cosh(K) - 2K\sinh(K) + 2\cosh(K) - 2}{K^4\cosh(K)} \quad (37c)$$

From eqn (36), the exact solution of the streaming potential is determined from eqn (38),

$$\bar{E}_x = \frac{(1 + b_{1/2}) - \sqrt{(1 + b_{1/2})^2 - 4a_{1/2}c_{1/2}}}{2a_{1/2}} \quad (38)$$

One can readily verify that the two results given by eqns (35) and (38) can be recovered from the general solution (eqn (35)) as special cases when *n* respectively equals 1 and ½.

5. APPARENT VISCOSITY AND ELECTROVISCOUS EFFECTS

In analogy to the expression for the volumetric flow rate of the classical Poiseuille flow, we define an apparent viscosity μ_a to express the volumetric flow rate as

$$Q_p = \frac{2H^3}{3\mu_a}(-\frac{dp}{dx}) \quad (39)$$

Eqn (39) can be nondimensionalized to

$$\bar{Q}_p = \frac{1}{3}\frac{V}{V_0}\frac{\rho VH}{\mu_a}(-\bar{P}_x) \quad (40)$$

Substituting eqn (24) and eqn (25) respectively into eqn (40), we can obtain the apparent viscosities of power-law fluids

$$\mu_a = \frac{\rho VH}{3}\frac{V}{V_0}\frac{-\bar{P}_x}{\bar{Q}} \quad \text{with consideration of the } \textit{electrokinetic} \text{ effects} \quad (41)$$

$$\mu_{a0} = \frac{\rho VH}{3}\frac{V}{V_0}\frac{-\bar{P}_x}{\bar{Q}_0} \quad \text{without consideration of the } \textit{electrokinetic} \text{ effects} \quad (42)$$

Then the ratio of the apparent viscosity with *electrokinetic* effects to that without *electrokinetic* effects is

$$\frac{\mu_a}{\mu_{a0}} = \frac{\bar{Q}_0}{\bar{Q}} \quad (43)$$

Eqn (43) can be used to characterize the electroviscous effect. From a physics viewpoint, this ratio should be always larger than unit one.

6. FRICTION COEFFICIENT

The friction factor for the flow through a channel is defined as

$$f = \frac{-\frac{dP}{dx}D_h/4}{\rho V_{av}^2/2} = 2\frac{-\bar{P}_x}{\bar{V}_{av}^2} \tag{44}$$

where D_h is the hydrodynamic diameter and $D_h = 4H$ for the present microchannel slit. Therefore, the friction coefficient, i.e., the product of the friction factor f and Reynolds number, is given by

$$C_f = f\,\mathrm{Re} = 2\left(\frac{n+1}{n}\frac{4}{\bar{V}_{av}}\right)^n \tag{45}$$

where the Reynolds number is defined as $\mathrm{Re} = \rho V_{av}^{2-n} D_h^n / m$.

7. RESULTS AND DISCUSSION

Examination of the afore-derived analytical expressions reveals that the characteristics of power-law fluids flow in a microchannel slit are determined by the four dimensionless parameters: K, $\bar{P}_x$, $\bar{G}_1$ and $\bar{G}_2$. Physically, the non-dimensional electrokinetic diameter, $K = \kappa H$, represents the ratio of half channel height to the thickness of the *EDL*. By definition, the non-dimensional pressure gradient, $\bar{P}_x = \frac{H}{2}\frac{dp}{dx}/\frac{1}{2}\rho V^2$, can be interpreted as the ratio of the pressure energy to the kinetic energy. $\bar{G}_1 = 2zen_\infty/\rho V^2$ characterizes the ratio of the electrical energy of the solution to the mechanical kinetic energy. $\bar{G}_2 = 2zen_\infty HV/\lambda_t\zeta_0$ represents the ratio of the streaming current to the conduction current[12,13,14] .

In calculation, without other specifications the following parameters and constants are used: the slit channel height $2H$=20 μm and length L=2 cm, the relative permittivity $\varepsilon_r = 80$, the absolute temperature T=300 K, the valence of ions $z_+ = -z_- = z = 1$, the wall zeta potential $\psi_w = -70$ mV, the ionic number concentration, 6.022×10^{20}/m^3, the fluid consistency index m=0.90×10^{-3} Pa$\cdot$s^n, and the pressure difference $\Delta p = 20$ kPa.

It should be pointed out that from the definitions of all the auxiliary functions in Appendix, they all have a singular point at $x = 0$. Therefore, in the calculations the limit values when x approaches to zero are used to evaluate their values at $x = 0$.

7.1 Velocity distribution

Figure 2 shows the dimensionless velocity distributions (valuated using eqn (20) with the centerline velocity in the absence of the *EDL* effects as the reference velocity given in eqn (12)) for three different flow behavior index of power-law fluids. In Figure 2(a)-(c), the dimensionless velocity distributions of power-law fluids without the electrokinetic effects are also plotted in dotted lines for comparison. As seen from the figures, the *EDL* exhibits stronger effects on the velocity distributions with lower flow behavior index than that with higher fluid behavior index. For a small fluid behavior index in Figure 2(a), the velocity distribution is distorted and the flow velocity approaches zero in the neighborhood of the channel wall region due to the action of the *EDL* field and the induced streaming potential. Meanwhile, the velocity at the channel centerline is significantly reduced. As the fluid behavior index is increased (e.g., Figure 2(b)), the distortion becomes smaller. In Figure 2(c) where the fluid behavior index is n=1.2, the difference of the velocity distributions with and without consideration of the electrokinetic effects become indistinguishable, indicating negligible electrokinetic effects in this case. In addition, as revealed by Figure 2(a) and 2(b), changing flow behavior index from 1 to 0.8 can increase one order of magnitude of the velocity, suggesting that the magnitude of velocity for pseudoplastic fluids (i.e., n<1) is very sensitive to the flow behavior index. Hence this feature may be able to be used as an effective way to adjust the flow rate in practical applications.

(a)

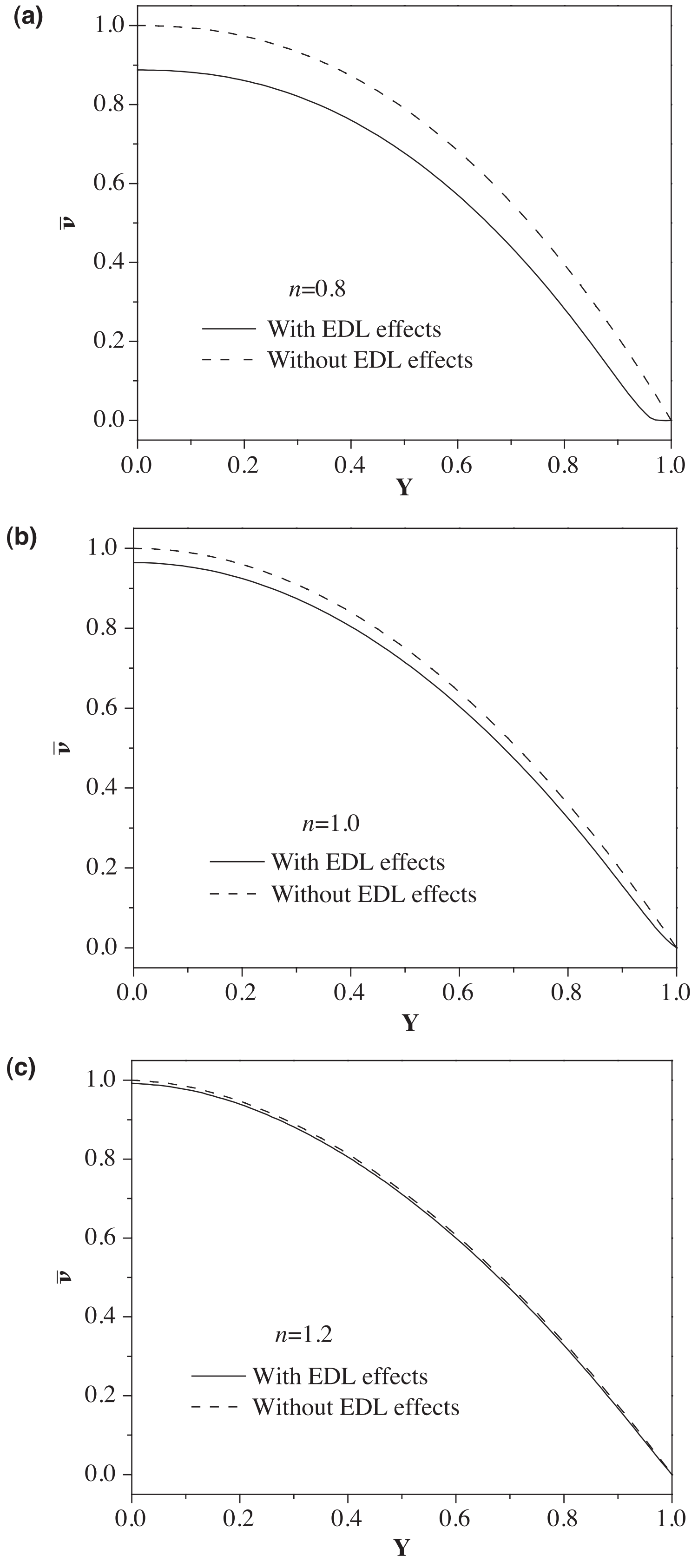

Figure 2. Non-dimensional Velocity distributions for three different flow behavior index (a) n=0.8; (b) n=1.0; and (c) n=1.2. The solid lines represent the cases with *EDL* effects and the dotted lines denote the cases without *EDL* effects. Other parameters are the wall zeta potential $\psi_w = -70mV$, the ionic concentration $n_\infty = 6.022 \times 10^{20}/m^3$, and the applied pressure difference Δp=10kPa.

7.2 Non-dimensional induced streaming potential

Figure 3 shows the non-dimensional induced streaming potential (calculated from eqn (32)) versus the flow behavior index for three different pressure differences. As elaborated earlier, in pressure-driven flow a streaming potential is induced along the channel axial direction due to the presence of the channel *EDL*. Therefore, a larger pressure difference can cause a larger amount of fluid transport and hence more ions are carried to the downstream end of the channel, giving rise to a stronger (more negative) induced electrokinetic potential. Also, it is shown that under the same pressure difference, the streaming potential is larger for the pseudoplastic fluids than for the dilatants fluids (i.e., $n > 1$). Once the fluid behavior index is very large, say $n > 1.3$, no streaming potential is generated regardless of the difference in applied pressure.

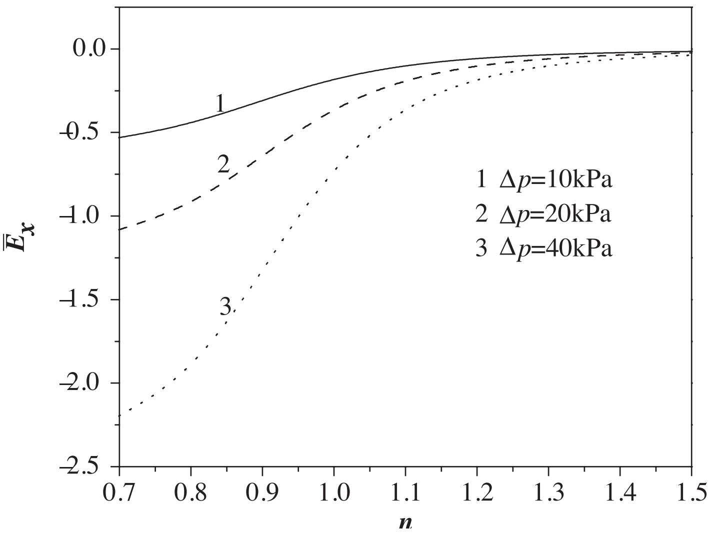

Figure 3. Non-dimensional streaming potential versus flow behavior index for three different pressure differences Δp=10kPa, 20kPa, and 40kPa. Other parameters are the wall zeta potential $\psi_w = -70mV$ and the ionic concentration $n_\infty = 6.022 \times 10^{20}/m^3$.

7.3 Volumetric flow rate

In Figure 4, the non-dimensional volumetric flow rate is plotted as a function of the flow behavior index for two different wall zeta potentials and pressure differences. As expected, the volumetric flow rate decreases with increasing the flow behavior index. For large flow behavior index of dilatants fluids, e.g., $n>1.3$, the fluids become so viscous so that no flow occurs under such applied pressures. Also, the electrokinetic effects are observed only in the pseudoplastic fluids, i.e., $n<1$. The consequence of electrokinetic effects is a reduction of flow rate, and such electrokinetic effects are stronger for a larger applied pressure difference or/and higher channel zeta potential.

7.4 Apparent viscosity (electroviscous effects)

The ratio of the apparent viscosity (defined by eqn (43)) with the *EDL* effects to that without consideration of the *EDL* effects is presented in Figure 5 which shows this ratio versus the flow behavior index for four different electrokinetic parameters. For a small electrokinetic parameter of K=10, it is noticeable that the electroviscous effect is present in almost the entire range of the flow behavior index range studied here. Specifically, the apparent viscosity ratio can be 2.5 times for a pseudoplastic fluid of n=0.6. As K increases, the range of fluids (characterized by the flow behavior index) where electroviscous effects are present shrinks significantly. Since increasing K either means an increase of the *EDL* thickness or a decrease of the channel height, both reduce the predominance of the *EDL* in the flow domain, resulting in weaker electroviscous effects. In a limiting case of K=100, the ratio μ_a / μ_{a0} becomes unity one, indicating that no electroviscous effects can be observed irrespective of the flow behavior index.

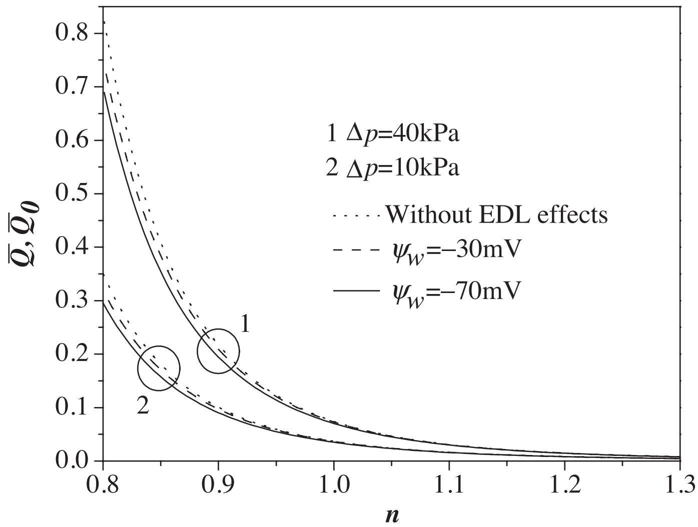

Figure 4. Non-dimensional volumetric flow rate versus flow behavior index for two different pressure differences (Δp=10kPa and 40kPa) and two zeta potentials (ψ_w=–30mV and –70mV).

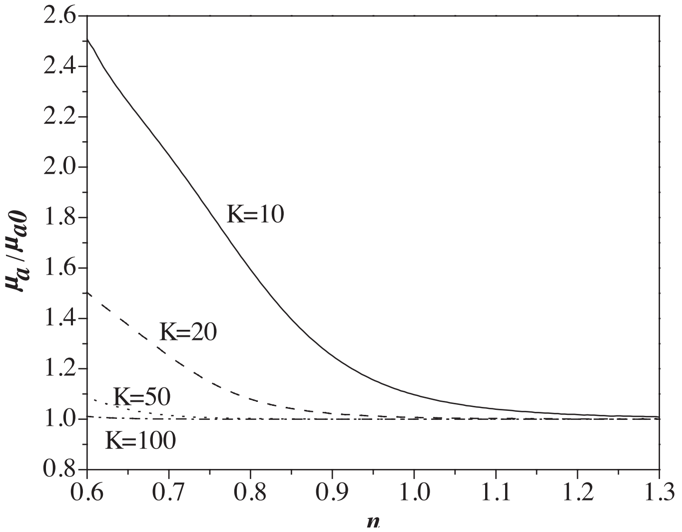

Figure 5. Variation of μ_a/μ_{a0} with flow behavior index for four different electrokinetic parameters K with an applied pressure difference Δp=20kP and a wall potential ψ_w=–70mV.

7.5 Friction Coefficient

Figure 6 depicts variation of the friction coefficient, expressed by eqn (45) with the flow behavior index for three different bulk ionic number concentrations. The general trend is that the friction coefficient increases with increasing the flow behavior index. Also, a well-known friction coefficient of 24 for Newtonian fluids without electrokinetic effects is retrieved in this figure. All these coincide with our expectations.

Figure 6 shows that the friction coefficient with *EDL* effects is always larger than that without *EDL* effects. The electrokinetic effects intensify as the ionic concentration decreases. Astonishingly, for a concentrated solution of n_∞=6.022×10^{23}/m^3, the electrokinetic effects vanish. As shown in the definition of $\kappa^{-1} = (\varepsilon k_B T / 2e^2 z^2 n_\infty)^{1/2}$, a decrease of ionic concentration leads to a thicker *EDL*, and thus the *EDL* exhibits stronger effects. Moreover, decreasing ionic concentration elevates the friction coefficient in the pseudoplastic domain more remarkably than that in the dilatant domain. This feature can also be ascribed to the fact that the pseudoplastic fluids are more sensitive to the hindrance of electroviscous effects.

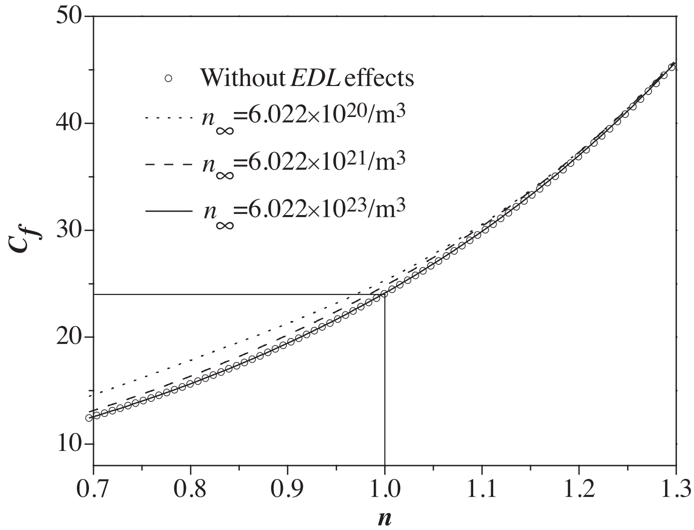

Figure 6. Variation of friction coefficient with flow behavior index for three different bulk ionic concentrations n_∞=6.022×10^{20}/m^3, 6.022×10^{21}/m^3 and 6.022×10^{23}/m^3 with an applied pressure difference Δp=20kPa and a wall zeta potential ψ_w=–70mV.

8. CONCLUSIONS

The electrokinetic effects on the liquid flow of power-law fluids through a microchannel slit are studied analytically. An electrostatic body force is considered in the Cauchy momentum equation governing the flow behavior of power-law fluids to account for the electrokinetic effects caused by the interaction of the channel wall *EDL* field and the induced streaming potential. The analytical solutions to the Cauchy momentum equation is obtained by using an approximate scheme. The expressions for the streaming potential, velocity distribution, volumetric flow rate, apparent viscosity and friction coefficient are derived. The computational results show that the electrokinetic effects result in the velocity distribution distortion, and thus cause stronger retarded flow of power-law fluids with smaller behavior index. Small dimensionless electrokinetic diameters or dilute ionic concentrations can leads to stronger electrokinetic effects, giving rise to larger apparent viscosity ratio and higher friction coefficient. Overall, the electrokinetic effects in the pseudoplastic domain are more remarkable than in the dilatant domain.

ACKNOWLEDGEMENTS

The authors gratefully acknowledge the financial support from the Ministry of Education of Singapore to CY (RG17/05) and the Ph.D. scholarship from Nanyang Technological University to CLZ.

APPENDIX

In the following, we will define several auxiliary functions which facilitate the analytical evaluation of the pertinent expressions in the present work. All these functions are obtained through integrations and are found to have a combination of the incomplete Gamma function.

$$\begin{aligned} F(n,x) &= \int x^{-1+\frac{1}{n}} \sinh(x)\,dx \\ &= \frac{1}{2}[\Gamma(\frac{1}{n},x) - (-x)^{-\frac{1}{n}} x^{\frac{1}{n}} \Gamma(\frac{1}{n},-x)] \end{aligned} \tag{A1}$$

$$\begin{aligned} F_1(n,x) &= \int F(n,x)\,dx \\ &= \frac{1}{2}[x^{1+\frac{1}{n}}\Gamma(1+\frac{1}{n},-x)(-x)^{-1-\frac{1}{n}} - \Gamma(1+\frac{1}{n},x) + x\Gamma(\frac{1}{n},x) - (-x)^{-1/n} x^{1+1/n}\Gamma(\frac{1}{n},-x)] \end{aligned} \tag{A2}$$

$$
\begin{aligned}
F_2(n,x) &= \int F(n,x)\cosh(x)dx \\
&= 2^{-1-\frac{n+1}{n}}(-x)^{-1/n}\{x^{\frac{1}{n}}\Gamma(\frac{1}{n},-2x) + \\
&+(-x)^{\frac{1}{n}}\Gamma(\frac{1}{n},2x)2^{1+\frac{1}{n}}[n(-x^2)^{\frac{1}{n}} - x^{\frac{1}{n}}\Gamma(\frac{1}{n},-x)\sinh(x) + (-x)^{\frac{1}{n}}\Gamma(\frac{1}{n},x)\sinh(x)]\}
\end{aligned} \tag{A3}
$$

$$
\begin{aligned}
F_3(n,x) &= \int x^{1+\frac{1}{n}}\cosh(x)\,dx \\
&= -\frac{1}{2}\{(-x)^{-\frac{1}{n}}x^{\frac{1}{n}}\Gamma(2+\frac{1}{n},-x)+\Gamma(2+\frac{1}{n},x)\}
\end{aligned} \tag{A4}
$$

$$
\begin{aligned}
H(n,x) &= \int x^{-2+\frac{1}{n}}\sinh^2(x)dx \\
&= \frac{1}{2}[\frac{nx^{-1+\frac{1}{n}}}{-1+n} + 2^{-1/n}(-x)^{-1/n}x^{1/n}\Gamma(-1+\frac{1}{n},-2x) - 2^{-1/n}\Gamma(-1+\frac{1}{n},2x)]
\end{aligned} \tag{A5}
$$

$$
\begin{aligned}
H_1(n,x) &= \int H(n,x)\,dx \\
&= \frac{1}{2}\{2^{-1/n}(-x)^{-1/n}x^{1/n}[x\Gamma(-1+\frac{1}{n},-2x)+\frac{1}{2}\Gamma(\frac{1}{n},-2x)] - \\
&- 2^{-1/n}[x\Gamma(-1+\frac{1}{n},2x) - \frac{1}{2}\Gamma(\frac{1}{n},2x)] + \frac{n^2x^{1/n}}{n-1}\}
\end{aligned} \tag{A6}
$$

$$
\begin{aligned}
H_2(n,x) &= \int H(n,x)\cosh(x)dx \\
&= \frac{1}{8}\{(-x)^{-1/n}x^{1/n}[\Gamma(-1+\frac{1}{n},-x) - 3^{-\frac{1+n}{n}}\Gamma(-1+\frac{1}{n},-3x) + 2^{-\frac{1}{n}+2}\Gamma(-1+\frac{1}{n},-2x)\sinh(x)] - \\
&- [-\Gamma(-1+\frac{1}{n},x) + 3^{\frac{-1+n}{n}}\Gamma(-1+\frac{1}{n},3x) + 2^{-\frac{1}{n}+2}\Gamma(-1+\frac{1}{n},2x)\sinh(x)] + \\
&+ \frac{2n}{(-1+n)}[-(-x)^{-1/n}x^{\frac{1}{n}}\Gamma(\frac{1}{n},-x) - \Gamma(\frac{1}{n},x)]\}
\end{aligned} \tag{A7}
$$

where $\Gamma(\alpha, \xi)$ is the incomplete Gamma function.

REFERENCES

1. Ho, C.M. and Tai, Y.C., Micro-electro-mechanical-systems (MEMS) and Fluid Flow, *Annual Review of Fluid Mechanics*, 1998, 30, 579–612.
2. Bousse, L., Cohen, C., Nikiforov, T., Chow, A., Kopf-Sill, A.R., Dubrow, R. and Parce, J.W., Electrokinetically Controlled Microfluidic Analysis Systems, *Annual Review of Biophysics and Biomolecular Structure*, 2000, 29, 155–181.
3. Eringen, A. C., Theory of Micropolar Fluids, *Journal of Mathematics and Mechanics*, 1966, 16, 1–18.
4. Migun, N. P. and Prokhorenko, P. P., Measurement of Viscosity of Polar Liquids in Microcapillaries, *Colloid Journal of the USSR*, 1987, 49, 894–897.
5. Rice, C. L. and Whitehead, R., Electrokinetic Flow in a Narrow Cylindrical Capillary, *Journal of*

Physical Chemistry, 1965, 69, 4017–4024.

6. Mala, G.M., Li, D., Werner, C. and Jacobasch, H.J., Flow Characteristics of Water through a Microchannel between Two Parallel Plates with Electrokinetic Effects, *International Journal of Heat and Fluid Flow*, 1997, 18, 489–496.
7. Ren, L. Li, D. and Qu, W., Electroviscous effects on Liquid Flow in Microchannels, *Journal of Colloid and Interface Science*, 2001, 233, 12–22.
8. Kulinsky, L., Wang, Y. and Ferrari, M., Electroviscous Effects in Microchannels, in: Ferrari, M., ed., *Micro- and Nanofabricated Structures and Devices for Biomedical Environmental Applications II*(*Vol.3606*): *Proceedings of SPIE*, California, 1999, 158–168.
9. Brutin, D. and Tadrist, L., Experimental Friction Factor of a Liquid Flow in Microtubes, *Physics of Fluids*, 2003, 15, 653–661.
10. Mala, G.M., Li, D. and Dale, J.D., Heat Transfer and Fluid Flow in Microchannels, *International Journal of Heat Mass Transfer*, 1997, 40, 3079–3088.
11. Chun, M. and Kwak, H.W., Electrokinetic Flow and Electroviscous Effect in a Charged Slit-like Microfluidic Channel with Nonlinear Poisson-Boltzmann Field, *Korea-Australia Rheology Journal*, 2003, 15, 83–90.
12. Yang, C. and Li, D., Electrokinetic Effects on Pressure-driven Liquid Flows in Rectangular Microchannels, *Journal of Colloid and Interface Science*,1997, 194, 95–107.
13. Yang, C. and Li, D., Analysis of Electrokinetic Effects on the Liquid Flow in Rectangular Microchannels, *Colloids and Surfaces A: Physicochemical and Engineering Aspects*, 1998, 143, 339–353.
14. Yang, C., Li, D. and Masliyah, J.H., Modeling Forced Liquid Convection in Rectangular Microchannels with Electrokinetic Effects, *International Journal of Heat Mass Transfer*, 1998, 41, 4229–4249.
15. Kamisli, F., Flow Analysis of a Power-Law Fluid Confined in an Extrusion Die, *Intentional Journal of Engineering Science*, 2003, 41, 1059–1083.
16. Zimmerman, W.B., Rees, J.M. and Craven, T.J., Rheometry of Non-Newtonian Electrokinetics Flow in Microchannel T-junction, *Microfluidics and Nanofluidics*, 2006, 2, 481–492.
17. Koh, Y.H., Ong, N.S., Chen, X.Y., Lam, Y.C. and Chai, J.C., Effect of Temperature and Inlet Velocity on the Flow of a Non-Newtonian Fluid, *International Communications in Heat and Mass Transfer*, 2004, 31,1005–1013.
18. Das, M., Jain, V.K. and Ghoshdastidar, P.S., Fluid Flow Analysis of Magnetorheological Abrasive Flow Finishing (MRAFF) Process, *International Journal of Machine Tools and Manufacture*, 2008, 48, 415–426.
19. Das, S. and Chakraborty, S., Analytical Solutions for Velocity, Temperature and Concentration Distribution in Electroosmotic Microchannel Flows of a Non-Newtonian Bio-Fluid, *Analytica Chimica Acta*, 2006, 559, 15–24.
20. Berli, C.L.A. and Olivares, M.L., Electrokinetic Flow of Non-Newtonian Fluids in Microchannels, *Journal of Colloid and Interface Science*, 2008, 320, 582–589.
21. Zhao, C., Zholkovskij, E., Masliyah, J. H. and Yang, C., Analysis of Electroosmotic Flow of Power-law Fluids in a Slit Microchannel, *Journal of Colloid and Interface Science*, 2008, 326, 503–510.
22. Deen, W.M., *Analysis of Transport Phenomena*, Oxford University Press, New York, 1998.
23. Masliyah, J. H. and Bhattacharjee, S., *Electrokinetic and Colloid Transport Phenomena*, John Wiley & Sons, New Jersey, 2006.